INTERNATIONAL JOURNAL OF HYDROGEN ENERGY 42 (2017) 2771–2789

Available online at www.sciencedirect.com

ScienceDirect

journal homepage: www.elsevier.com/locate/he

Conceptual design, process integration, and optimization of a solar Cu–Cl thermochemical hydrogen production plant

Hoseyn Sayyaadi[*], *Milad Saeedi Boroujeni*

Faculty of Mechanical Engineering-Energy Division, K.N. Toosi University of Technology, P.O. Box: 19395-1999, No. 15-19, Pardis St., Mollasadra Ave., Vanak Sq., Tehran 1999 143344, Iran

ARTICLE INFO

Article history:
Received 28 August 2016
Received in revised form
7 December 2016
Accepted 8 December 2016
Available online 4 February 2017

Keywords:
Solar thermochemical Cu–Cl cycle: heat recovery
Pinch analysis
Exergoeconomic analysis
Multi-criteria optimization
Decision-making

ABSTRACT

A conceptual design of a solar Cu–Cl thermochemical cycle with the capacity of 6000 kg day^{-1} was presented. To enhance thermal efficiency, the heat recovery within Cu–Cl thermochemical hydrogen production cycle was proposed using the pinch analysis to design a heat exchanger network that recovers heat between hot and cold streams. This improves +10.2% in the thermal efficiency of the cycle compared to previous designs. The reformed cycle was assumed to be coupled to a solar installation that provides the required thermal energy for the cycle. For further improvement, the conceptual design was considered as the base case and four optimization scenarios were conducted on that. Three objective functions, including energy efficiency, exergy efficiency and the unit cost of hydrogen were optimized in three single-objective and one multi-objective scenario. Comprehensive thermodynamic, solar thermal, and exergoeconomic models were employed to obtain objective functions. Reaction temperatures, the number of the solar collectors, and volume of the solar storage tank were selected as design variables. The best alternative to five systems (one base case and four optimized systems) were selected using the TOPSIS method. It was found that thermal efficiency-optimized system has the preference over other four systems. It had 49.83% thermal efficiency, 58.23% exergetic efficiency and 6.33 $ kg^{-1} for produced hydrogen.

Introduction

For many years, hydrogen has been considered as an important energy carrier due to its high calorific value, which is even more than fossil fuels, i.e. about 120 GJ ton^{-1} [1]. Hydrogen can be stored effortlessly and then utilized in the essential place. Since the early 1970s, research on the water splitting into its constituent elements (H_2 and O_2) has been started [1]. In addition, hydrogen has the potential of being used as a fuel to generate electricity, thermal energy or in transportation. After releasing its energy by combustion, water and heat are produced as two outcomes. A comparative review of various aspects of different hydrogen production cycles was given by Nikolaidis and Poullikkas [2]. If a clean and renewable energy could be used in splitting water to produce hydrogen, no greenhouse-gas emissions, and environmental pollution in production and consumption of the hydrogen would be

* *Corresponding author*. Fax: +98 21 8867 4748.
E-mail addresses: sayyaadi@kntu.ac.ir, hoseynsayyaadi@gmail.com (H. Sayyaadi).
http://dx.doi.org/10.1016/j.ijhydene.2016.12.034
0360-3199/

Nomenclature

a	empirical coefficient for solar calculation
b	empirical coefficient for solar calculation
c	the unit cost of an exergy stream, \$ kJ^{-1}
E	electric energy
$\overline{Ex}_d$	exergy destruction of the plant per mole of generated hydrogen, kW mol^{-1}
$\dot{E}x$	exergy rate, kW
ex	specific exergy, kJ kmol^{-1}
$\overline{h}$	specific molar enthalpy, kJ kmol^{-1}
$\overline{h}^{o}$	specific molar enthalpy at reference state, kJ kmol^{-1}
$\overline{h}_f^{o}$	enthalpy of formation, kJ kmol^{-1}
hs	solar hours angle, °
I	beam intensity, kW m^{-2}
k_T	clearness index
L	latitude
$\overline{LHV}$	molar lower heat value, kJ kmol^{-1}
$\dot{m}$	mass flow rate, kg s^{-1}
N	a counter index for days during a year
$\dot{n}$	molar flow rate, kmol s^{-1}
PEC	purchase equipment cost, \$
$\dot{Q}$	heat transfer rate, kW
S	stored thermal energy, kJ
s	specific entropy, kJ kmol^{-1} K^{-1}
s^{o}	specific entropy at reference state, kJ kmol^{-1} K^{-1}
t	time, s or h
T_0	reference-environment temperature, °C or K
T	temperature, °C or K
TRR	total revenue requirement
$\dot{Z}_k$	the total cost rate of kth component including capital investment and operating-maintenance cost, \$ h^{-1}

Greek letters

α	solar altitude angle, °
β	inclination angle of the collector surface, °
Δ	finite change in a quantity
δ_s	solar declination angle, °
$\eta_{th,\ overall}$	energy (thermal) efficiency of the plant, %
$\eta_{ex,\ overall}$	exergy efficiency of the plant, %
τ	annual operating hours, h
Φ	received solar thermal energy, kJ

Subscripts

0	reference state
a	average
c	cold
ce	common equity
CI	capital investment
d	destruction, debt
e	exit (outlet)
h	hot
i	inlet
k	kth component
min	minimum
ps	preferred stock
$pinch$	pinch
q	thermal
$reac$	reaction
sys	system
$step1,2,3,4,5$	related to reaction step 1–5 in CCC
w	power

Superscripts

$\cdot$	quantity per unit time
°	standard reference-state
CH	chemical
PH	physical
OM	operating and maintenance

Acronyms

CCC	Cu–Cl cycle

created. More than 99% of the hydrogen consumption in industries is achieved from fossil fuels and crude oil. By the reason, investments have been done to find other sources to produce hydrogen. Hence, at the moment more than 800 thermo-chemical cycles are being proposed for producing hydrogen from water as a raw material [1]. A number of these cycles are currently used for small-scale hydrogen production and some of them are not effective, economically. The thermo-chemical cycle involves a series of chemical processes, which is resulted from a combination of water and heat to produce H_2 and O_2. One of the positive points of thermo-chemical cycles is being more efficient and cost-effective compared with other methods. However, there are limited number of thermo-chemical hydrogen production cycles which are used on an industrial scale due to their high-temperature requirements (about 850–900 °C). One of the most successful cycles in producing hydrogen is a Cu–Cl cycle. In this cycle, the required temperature is about 530 °C. Due to its lower required temperature, Cu–Cl cycle (CCC) can be coupled with small nuclear reactors; renewable energy such as solar or waste heat from the exhaust of gas turbine for providing essential heat for reactions. On the other side of researches, a comparative assessment of different chlorine family was given by Tolga Balta et al. [3]. They compared copper-chlorine (CuCl), magnesium-chlorine (MgCl), iron-chlorine (FeCl) and vanadium-chlorine (VeCl) cycles from the energy and exergy analysing aspects. They showed that the VCl cycle was one of the most promising low-temperature cycles due to a high efficiency, over 40% and the concluded that it competes with other low-temperature cycles such as the CuCl cycle. Nevertheless, the CuCl cycle is still among the most promising thermochemical cycles that is paid attention by many researchers nowadays.

In CCC, through a series of chemical reactions with the interference of chlorine and copper compounds, water is decomposed into hydrogen and Oxygen. Different steps of this cycle are (1) HCl production (2) O_2 production (3) Cu production (electrolysis of solid Cu–Cl) (4) drying of the slurry $CuCl_2$ (5) H_2 production, respectively. Except drying step, in other steps, a chemical reaction will be occurred as presented in Table 1. CCC includes of three reactions; endothermic, exothermic and an electrolysis reaction. Chemical reactions form a closed

Table 1 – Primary steps in the Cu–Cl cycle with the corresponding reactions at 101 kPa [5].

Step	Reactions	Reaction type	Temperature range (°C)
1	$2CuCl_2(s) + H_2O(g) \rightarrow Cu_2OCl_2(s) + 2HCl(g)$	Endothermic	400
2	$Cu_2OCl_2(s) \rightarrow 2CuCl(l) + ½\ O_2(g)$	Endothermic	500
3	$4CuCl(s) + H_2O(l) \rightarrow 2\ CuCl_2(aq) + 2Cu(s)$	Electrolysis	Ambient
4	$2CuCl_2(aq) \rightarrow 2CuCl_2(s)$	Physical drying	>100
5	$2Cu(s) + 2HCl(g) \rightarrow 2CuCl(l) + H_2(g)$	Exothermic	430–475

inner ring which results in continuous recycle of all the copper and chloride compounds. In this technique, no greenhouse gasses discharge into the environment. The possibility of all these reactions already was confirmed, experimentally [4].

Many aspects of CCC have been assessed by previous researchers. Considering of CCC as a block box, Orhan et al. [5–8] has had cost-effective studies. In this regard, a five-step Cu–Cl cycle was examined carefully and analyzed from the economic perspective of energy and exergy. In those studies, the cycle and chemical reactions were introduced in general and in different steps, those were checked from the energy and exergy point of views. In addition, the chemical reactions were assumed to be fully developed and the effects of temperature and pressure on their extent of reaction were ignored. In general, an economic analysis was conducted on this cycle; however, due to the lack of preliminary information for plant design, including data required in the selection of equipment, the cost estimation was performed based on the similar sulphur-iodine plant. Therefore, the results from this attempt could be considered as only an overall estimated cost for Cl–Cu thermo-chemical cycle plant. Lewis et al. [4] examined the three-steps of CCC and presented further details of the relevant equipment within the plant through modeling in Aspen Plus software. In addition, a more accurate economic analysis on CCC was accomplished. Furthermore, a comprehensive exergoeconomic and exergoenvironmental analysis, as well as multi-objective optimization, were given by Ozbilen et al. for a four-step CuCl cycle [9,10]. Based on the nuclear energy and CCC, the recent progress regarding hydrogen production in Canada was summarized by Naterer et al. [11]. In this study, details on the chemistry of the cycle are investigated in the laboratory scale. Afterward, the industrial scale has been introduced. Furthermore, a cost comparison for hydrogen production through different cycles with no explanation of the details of calculations has been presented. Daggupati et al. [12] discussed the impact of chemical process variables on the thermo-chemical cycles' reactions. In that research, a complete chemistry perspective and the effects of temperature on the progress of the chemical reactions were investigated, and reactions were analyzed individually without considering them in a closed loop. Momirlan and Magdalena [13] showed the current status of hydrogen energy and new developments in its production in his work. Process integration and heat recovery in CCC has been attentional by a number of researchers. In this regard, Rabbani et al. [14] specified parameters of heat exchangers for the most effective heat recovery in a Cu–Cl thermochemical hydrogen production cycle. In another work, Pope et al. [15] presented three integration pathways for the copper chloride flows between electrolysis and hydrolysis reactors in terms of energy saving and reduction of auxiliary operations for the processing of the flows. The solid precipitation of $CuCl_2$ using a crystallization process, water vaporization in the hydrolysis reactor by introducing the electrolyser outlet stream directly to the reactor, and vaporization in an intermediate spray dryer were suggested as the integration pathways. Wu et al. [16] provided the heat integration and economic analysis based on net present value (NPV) as well as the internal rate of return (IRR) of a three-step CuCl plant. They increased the overall efficiency of the plant from 33.87% to 47.31%. Moreover, they concluded that the massive production process can effectively reduce the production costs of hydrogen and oxygen if the pretreatment process for aqueous $CuCl_2$ is feasible, and its operating cost is lower than the feedstock cost of solid CuCl. To increase the efficiency of hydrogen production cycle hybrid systems are also suggested. In this regards, Jaszczur et al. [17] performed efficiency analysis of a combined cycle that includes a high-temperature nuclear reactor combined with a gas turbine, a steam turbine, and a system for delivering thermal energy into the hydrogen production cycle and increased the efficiency of the combined cycle up to 50%.

Besides, the high-temperature nuclear reactors, renewable energies were considered as low carbon emission thermal source to provide the required heat of thermochemical hydrogen production cycles. Wang et al. [18] performed some feasibility study of different methods of solar thermal energy absorption in various thermochemical cycles, including CCC, and concluded that using existing technologies, producing hydrogen in the cycle of Cu–Cl, with the aid of solar energy is possible. They have also introduced implication of various types of heat, which comes from the solar hot salt in different reactors to provide the required heat in different steps of the cycle.

Ghandehariun et al. [19] examined the coupling of a CCC with a solar thermal plant to provide required heat for the reactor of the oxygen production step. This reactor requires the highest temperature out of the whole cycle. They also tried to determine the number of parabolic trough collector pans as well as the size of storage tanks for holding hot and cold molten salt. The considered plant could produce 6000 kg of hydrogen per day for continuous production and supposed to be located in three cities in Canada. In another study, Ghandehariun et al. [20] evaluated and compared different methods for heat recovery from the molten Cu–Cl and concluded that the Casting/Extrusion and atomization method for Cu–Cl salt, especially in the presence of a cooling gas stream would be the best choice. Jaberet et al. [21] evaluated the heat recovery from the molten Cu–Cl in a direct contact air-cooled heat exchanger. Their studies were proposed from the perspective of convective heat transfer and obtained the optimum

diameter and length for the heat exchanger. Studies and comparison among different types of solar-based hydrogen production methods were presented by Yilmaz et al. [22]. In another work, Ghandehariun et al. [23] increased the heat recovery by controlling the size of molten salt droplets in a spray column. This work was used to enhance the overall efficiency within the CCC, using the smaller particle sizes, the greater heat transfer rate, and the smaller column height. Hosseini and Wahid [24] compared the cost of hydrogen production from a solar/wind base source with fossil fuel's base source. They found out as electricity costs are important in final hydrogen, for having hydrogen from renewable sources at a competitive price, the cost of electricity should be reduced. In the field of solar-hydrogen production, Ratlamwala and Dincer [25] presented a comprehensive exergy analysis of two solar based hydrogen production plant, including a solar heliostat system integrated with Cu–Cl cycle and Kalina cycle. A parametric study was conducted to investigate the effects of varying the operating conditions and system parameters on the performances of these integrated systems. The effects of variations in solar light intensity, ambient temperature, and mass flow rate of the ZnS on the hydrogen production rate and overall energy and exergy efficiencies were studied and presented comparatively. The results showed that hydrogen production rate and exergetic efficiency increased by a rise in solar light intensity. It was also observed that the rise of the ambient temperature had no effect on the energy efficiencies of systems but the exergy efficiencies of systems were increased. Finally, solar base hydrogen production methods were extensively reviewed by Yilmaz et al. [26]. Moreover, a similar review from the viewpoint of application of renewable energy in hydrogen production was reviewed by Dincer and Acar [27] and also by Terner et al. [28]. Application of other forms of renewable energies for the production of hydrogen was also studied. In this regard, a thermodynamic and thermoeconomic analysis of a geothermal-based energy based multi-generation cycle including a PEM electrolyzer was studied by Emri Yuksel and Ozturk [29].

The aim of this paper was to provide a preliminary conceptual design of the solar thermo-chemical CCC using the heat recovery through a heat exchanger network. The pinch technology was used to design a network that recovers the heat. Then modeling and multi-optimization of the proposed conceptual design of the cycle for increasing energy and exergy efficiency, increasing the production rate and reducing production cost were presented. For this purpose, first, a conceptual design of the Cu–Cl thermochemical cycle with the concept of heat recovery was presented. In this regard using pinch technology, a network of heat exchangers was designed to recover heat from cold and hot streams in the cycle. Thus, with increasing efficiency within the system; the required area of the solar collectors, as well as the size of the solar storage tank, would be decreased, significantly. The designed solar cycle was evaluated from the energy, exergy, economic and thermo-economic point of views, and it was finally optimized by selecting the appropriate decision variables. Temperatures of reactions in dissimilar reactors, the number of the solar collectors, and the volume of the molten salt tank were considered as decision variables of optimizations. These variables along with kinetic constraints to determine the allowable ranges of variables were considered as elements of optimization. In this regards, the multi-objective optimization algorithm known as NSGA-II was employed while the aims of optimization were increasing energy and exergy efficiency & productivity, and decreasing cost of production. These objectives were considered as the form of single-objective and multi-objective optimizations. In addition, the final optimum result in multi-objective optimization was chosen by the TOPSIS decision-making method. Finally, the capital cost and the cost of production per each kilogram of the produced hydrogen as well as energy and exergetic efficiency of different scenarios of the solar plant were compared. In summary, in comparison to literature about the Cu–Cl thermochemical cycle, in the current paper hole concepts of conceptual design, process integration, thermodynamic and thermoeconomic analysis, and multi-objective optimization were employed simultaneously to present a basic design of a Cu–Cl thermochemical cycle. In addition, employing the solar energy as a renewable source of thermal energy was considered to provide an environmentally friendly CCC plant. Moreover, a sophisticated economic model for estimating equipment cost and the unit cost of produced hydrogen was presented.

Conceptual design and heat recovery in the solar thermochemical cycle

In order to achieve an optimum heat exchanger network and maximum energy recovery, hot and cold streams existing in the cycle should be specified. Hot and cold streams are able to exchange heat with each other were evaluated and a heat exchanger network for recovering the heat was designed by the pinch analysis. The basic design of the system was based upon the production of 6000 kg the hydrogen per a day (3000 kmol per day).

Heat recovery potentials in the cycle

In thermo-chemical CCC, the molten salt of the copper–-chlorine (CuCl (l)) which is a product of reactors in the second (oxygen production) and fifth (hydrogen production) steps, should be cooled from the temperature of about 490 °C to about 25 °C. After solidification of CuCl, it should be entered in the third step with the cycle, i.e. electrolysis step. This process has the potential of heat release about 162 kJ kmol H_2^{-1} and has a significant potential for the heat recovery. It should be noted that converting liquid Cu–Cl to solid Cu–Cl using the conventional type of heat exchangers is impossible. Therefore, a special method like atomization or casting/extrusion shall be used [14]. In these two methods, water, air or other fluids like nitrogen can be used for heat exchange. Since the volume of the water is abruptly increased in evaporation, to prevent explosion danger of equipment, using the air or nitrogen instead of water was preferred [23].

The reactor of hydrogen production releases about 46.8 kJ kmol H_2^{-1} of heat at a temperature about 450 °C. In addition, the slurry of copper exited from the third step (electrolysis) shall be firstly warmed up to a temperature of

about 70 °C to be dried from the water. Then, before entering the fifth step reactor (hydrogen), the resulted copper particles shall be warmed up to a temperature of about 450 °C. For such elevated temperature, heating the copper, using conventional methods is impossible because the copper particles might react with oxygen from the air and oxidized consequently. Thus, depending on the type of drying process in the fourth step, the thermal energy could be provided in different ways. If in the fourth step, the spray flash method is applied to dry the slurry of $CuCl_2$ before receiving heat, thermal requirements of this step will be about 1360 kJ kmol H_2^{-1}, whereas using crystallization method to dry the slurry reduces heat requirements to about 554.7 kJ/kmol H_2 [25]. Hence, heating copper particles shall be performed in a neutral environment with a gas such as nitrogen or hydrogen at a temperature of 450 °C to avoid oxidization of the copper. Due to the presence of hydrogen in the cycle, heating copper particles with hydrogen can be effective economically. However, the flammability of hydrogen in this temperature range as well as its ignition without having a visible flame makes it as an undesired option. Therefore, generally rather than the direct usage of streams of the cycle, using the nitrogen as an intermediate fluid to recover heat in thermo-chemical CCC was recommended as follows:

First, the liquid CuCl is cooled by the nitrogen gas. The temperature can be decreased from 490 °C to 35 °C. Note that liquid copper chloride is produced in the fifth step of the cycle with the temperature of about 450 °C, first combines with copper chloride which produced in the second step of the cycle with temperature of 530 °C, and then with an average temperature of 490 °C enters into considered equipment to be cooled down. At this stage, the assumption is that temperature of the nitrogen rises from 25 °C to about 480 °C. In this process, 162 kJ kmol H_2^{-1} of the heat is exchanged between CuCl (l) and nitrogen gas.

In the next step, hot nitrogen gas heats the copper particles in an inert atmosphere from the temperature 70 °C to 450 °C and about 21 kJ kmol H_2^{-1} thermal energy is its outcome. As a result, the temperature of nitrogen is reduced to 411 °C. After that nitrogen gas can be utilized for a second time to heat and dry the slurry of produced copper from temperature of 35 °C to 70 °C for usage in the third step (electrolysis). Afterward, content water is evaporated and copper will re-enter the cycle and ultimately temperature of nitrogen gas after heating the slurry falls from 411 °C to about 323 °C. The nitrogen with the temperature of about 323 °C can be used to be enter to the heat exchangers network that was designed to recover its thermal energy to heat up other existing streams.

A part of heat requirements of the cycle (which is totally 554.7 kJ/kmol H_2) can be supplied by exothermic reactions and cooling processes of some streams within the cycle itself. According to the conducted analysis, it is possible to use the released heat during the fifth step (hydrogen production) and recovered heat from cooling process of the molten copper chloride salt (produced in second and fifth steps). As these reactions and processes occur at relatively high temperatures; the recovered thermal energy from them has a higher quality, making it as a suitable resource to be used in heating some other streams within the cycle.

Heat recovery and heat exchanger network design optimization

Fig. 1, was presented by Lewis et al. [30]; It demonstrates schematic of a conceptual design for the chlorine-copper thermochemical cycle.

As it is clear from Table 2, the streams #1, #2 and #3 (hydrogen, oxygen, and nitrogen) are the hot stream which required being cooled and the stream #4, #5 and #6 (water, solid $CuCl_2$and its slurries) are cold streams, which shall receive heat. The aim of optimum design of heat exchanger network using the pinch analysis is that not only the hot and cold streams can exchange heat with each other but also the maximum heat recovery occurs. In addition, pinch analysis is employed to minimize the hot and cold utilities required for heating of cold stream and cooling of hot streams, respectively. It also leads to the lowest rate of exergy destruction is the cycle. For this purpose, firstly, the composite curves should be drawn separately for the hot and cold streams. Then with a selection of the minimum temperature difference between two ends of the heat exchangers (in this study ΔT_{min} is considered 10 °C), the pinch point temperature was determined. Then the network of heat exchangers in both upper and lower parts of pinch point shall be designed.

Fig. 2 shows the composite curves for existing streams in the heat recovery network. The area between these two curves shows heat exchange limits and illustrates the amount of heat recovery. Fig. 3 shows a diagram of the energy cascade.

As shown in Fig. 3, the minimum hot utility required for heating the cold streams that cannot be heated up using the recovered heat was about 108.3 kJ kmol H_2^{-1}. Moreover, the minimum cold utility required for cooling the hot streams was about 4.11 kJ kmol H_2^{-1}, which is very negligible and at low temperatures. So, the ambient air can be used as a required cold utility. Also, the pinch point temperature gained from this diagram is 30 °C which can be used in heat exchanger network design. The heat exchanger network, HEN, related to recovering thermal heats between streams of Table 2 was illustrated in Fig. 4.

The minimum required heat for heating streams' number #4, #5 and #6 (water, solid $CuCl_2$ and its slurry) can be obtained by summing the values related with the heaters' number #4, #5 and #6 to each other, which gives 108.3 kJ kmol H_2^{-1}. Furthermore, the minimum cold utility requirement of the cooling stream number #1, #2 and #3 (hydrogen, oxygen, Nitrogen) can be obtained by adding values related with the coolers' number #7, #8 and #9, which are 4.11 kJ kmol H_2^{-1}. These values are exactly equal to the values obtained from composite curves and streams' energy cascade (Figs. 2 and 3). In addition, the amount of heat recovered from these streams is equivalent to 125 kJ kmol H_2^{-1} which can be achieved by summing the corresponding duties of the heat exchangers #1, #2 and #3.

On the other hand, the fifth step reactor in the cycle of hydrogen production, at a temperature about 450 °C, releases heat equal to 46.8 kJ kmol H_2^{-1} during the process. It can be used as part of required hot utility in the cycle (equal to 108.3 kJ kmol H_2^{-1}). For example, required heat by the stream number #4 (inlet water to the cycle) can be supplied

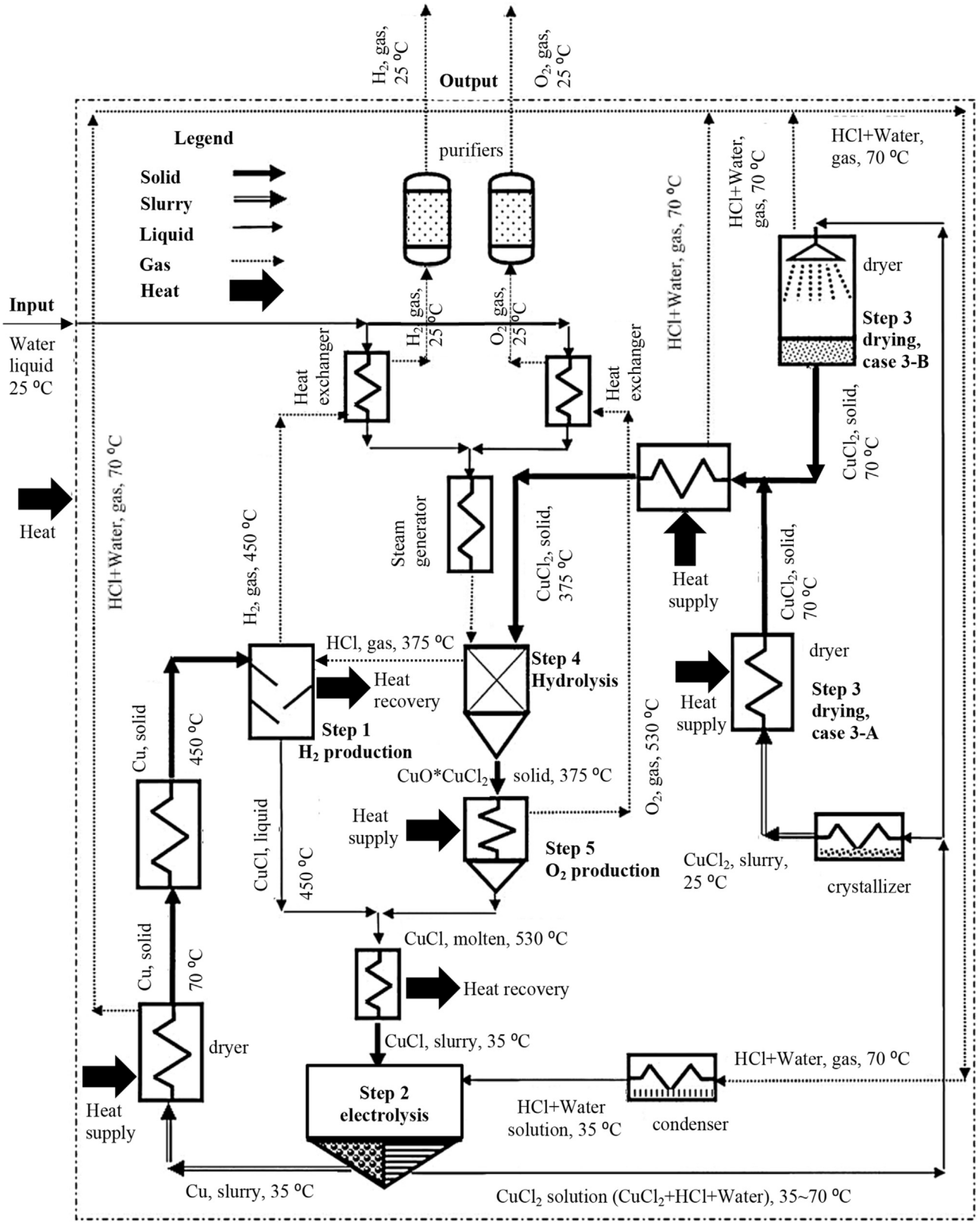

Fig. 1 – Hydrogen production via a five-step water-splitting thermochemical cycle based on Cu–Cl reactions [39].

Table 2 – List of hot/cold streams required for design and optimization [19].

Item	Component	T_1 (°C)	T_2 (°C)	ΔH (kJ mol^{-1} H_2)	C_P kJ mol^{-1} H_2^{-1}
1	H_2	450	25	12.2	0.029
2	O_2	530	25	7.4	0.0147
3	N_2	323	25	109.5	0.356
4	H_2O	25	375	57.1	0.163
5	$CuCl_2$(s)	70	375	47.2	0.155
6	$CuCl_2$(slurry)	25	70	129.0	2.866

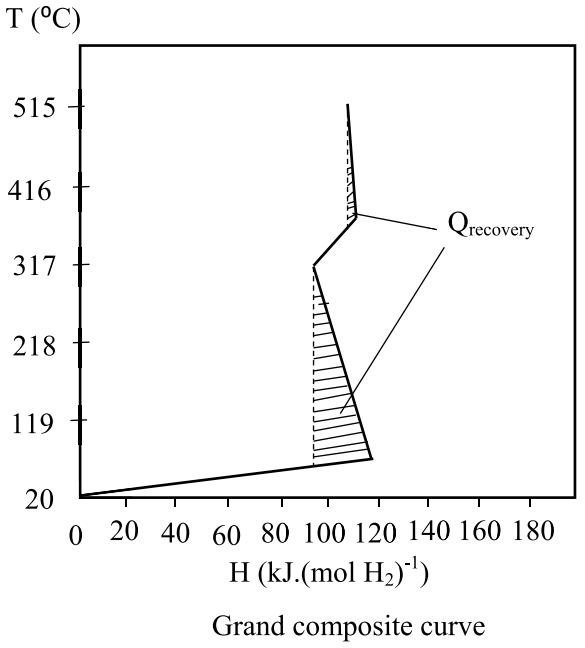

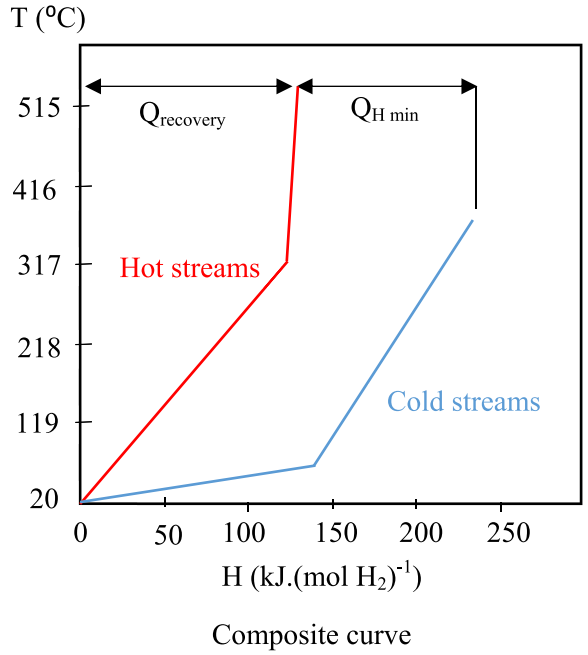

Fig. 2 – Grand composite and composite curves for the heat exchanger network.

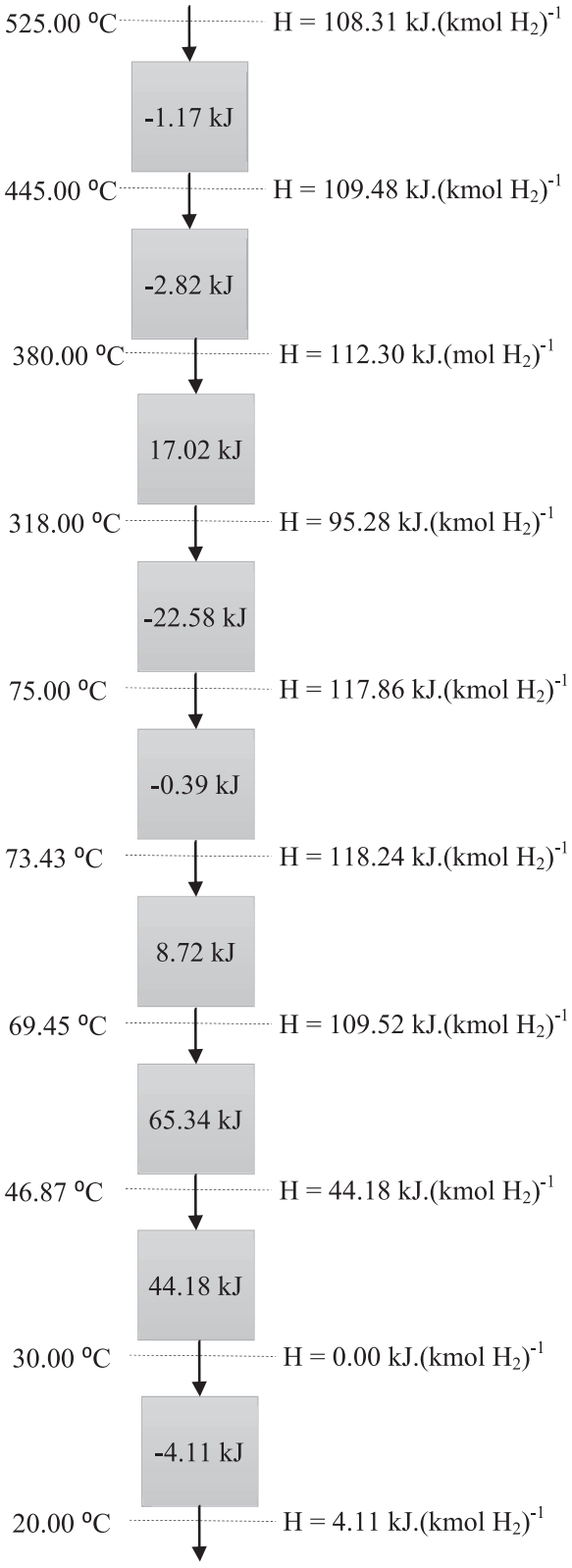

Fig. 3 – Cascade diagram of energy for hot/cold streams developed for the heat recovery in the proposed CCC plant (based on 1 mol of produced hydrogen).

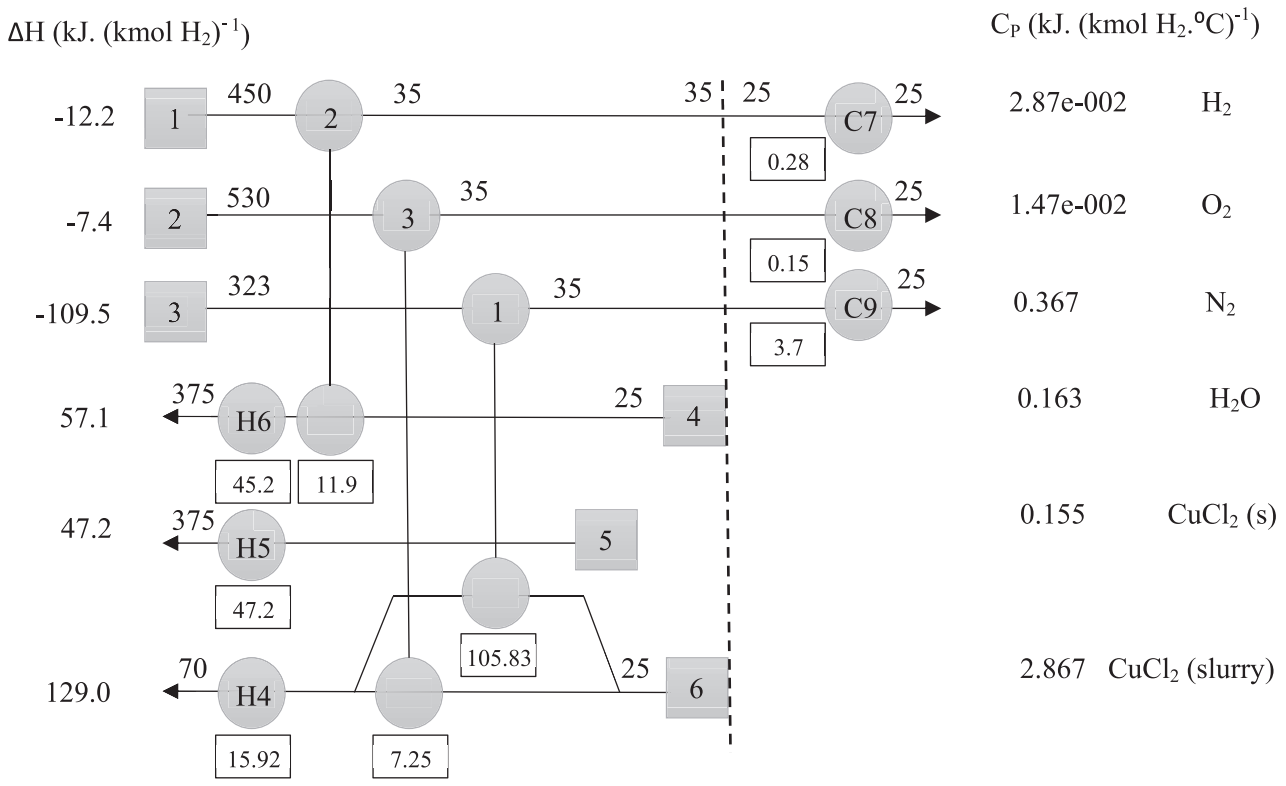

Fig. 4 – Heat exchanger network for the recovery of thermal energy within the CCC plant.

by this source. Thus, considering the amount of heat (21 kJ kmol H_2^{-1}) which is used for heating copper particles, the final amount of heat recovery from the sum of aforementioned values is equal to 192 kJ kmol H_2^{-1}.

This heat is used for:

- Heating the inlet water in the cycle for increasing its temperature to the temperature range of the first step reaction (hydrolysis)
- Drying of the slurry of $CuCl_2$ in the fourth step (drying)
- Drying of produced slurry of copper in the third step (electrolysis)
- Heating copper particles to enhance its temperature to the temperature of the fifth step reaction

By dividing the amount of the recovered heat to the total required heat of the cycle, the heat recovery efficiency is obtained:

$$\eta_{recovery} = \frac{Q_{recovery}}{Q_{Cycle}} = 0.391 \quad (1)$$

Hence, the heat recovery inside the cycle is about 39.1%, and the required amount of energy is about 361.9 kJ kmol H_2^{-1}. This amount contains the thermal energy required by the heat exchangers #4, #5, and #6, hydrolysis steps, oxygen production reactor (299.3 kJ kmol H_2^{-1}) and electrical energy required for electrolysis step (62.6 kJ kmol H_2^{-1}).

To provide the required heat for the cycle, it could be coupled with a solar thermal power plant. A stream such as molten salt is heated by the thermal energy from the sun. Then by transferring this salt to a thermo-chemical hydrogen cycle, the stored heat could be exchanged with those streams and reactors which are involving endothermic reactions. Finally, the molten salt is cooled and re-circulated to the solar installation.

Fig. 5 shows the schematic of modified Cu–Cl thermochemical cycle (after heat recovery) which is coupled with solar installations.

Specifications of streams that indicated in Fig. 5 was indicated in Table 3.

Fig. 5 illustrates that nitrogen gas is heated by the molten salt Cu–Cl initially. This enables nitrogen gas to heat the copper particles, copper slurry and a slurry of $CuCl_2$. After being cooled again, the nitrogen receives heat from the molten salt, and a closed cycle is repeated. Furthermore, in the fourth step, for the drying of the slurry of $CuCl_2$, the stream of $CuCl_2$ initially splits into two parts. One part of this stream is heated by the outlet oxygen gas from the second step, and the other part is heated by the nitrogen. These two slurry streams of $CuCl_2$ have joined together again and heated until reach to the desired temperature in the drying step, eventually. Furthermore, the solar molten salt after entering into the hydrogen production cycle provides the required heat of the second step (oxygen production). As mentioned earlier, this step operates at the highest temperature throughout the cycle. Afterward, the solar molten salt supplies the heat required for the first step of the cycle (hydrolysis) and then required heat for heating the solid $CuCl_2$ (exiting from the fourth step and entering to the first step) and eventually exits from the cycle. Another part of the required energy required by the Cu–Cl

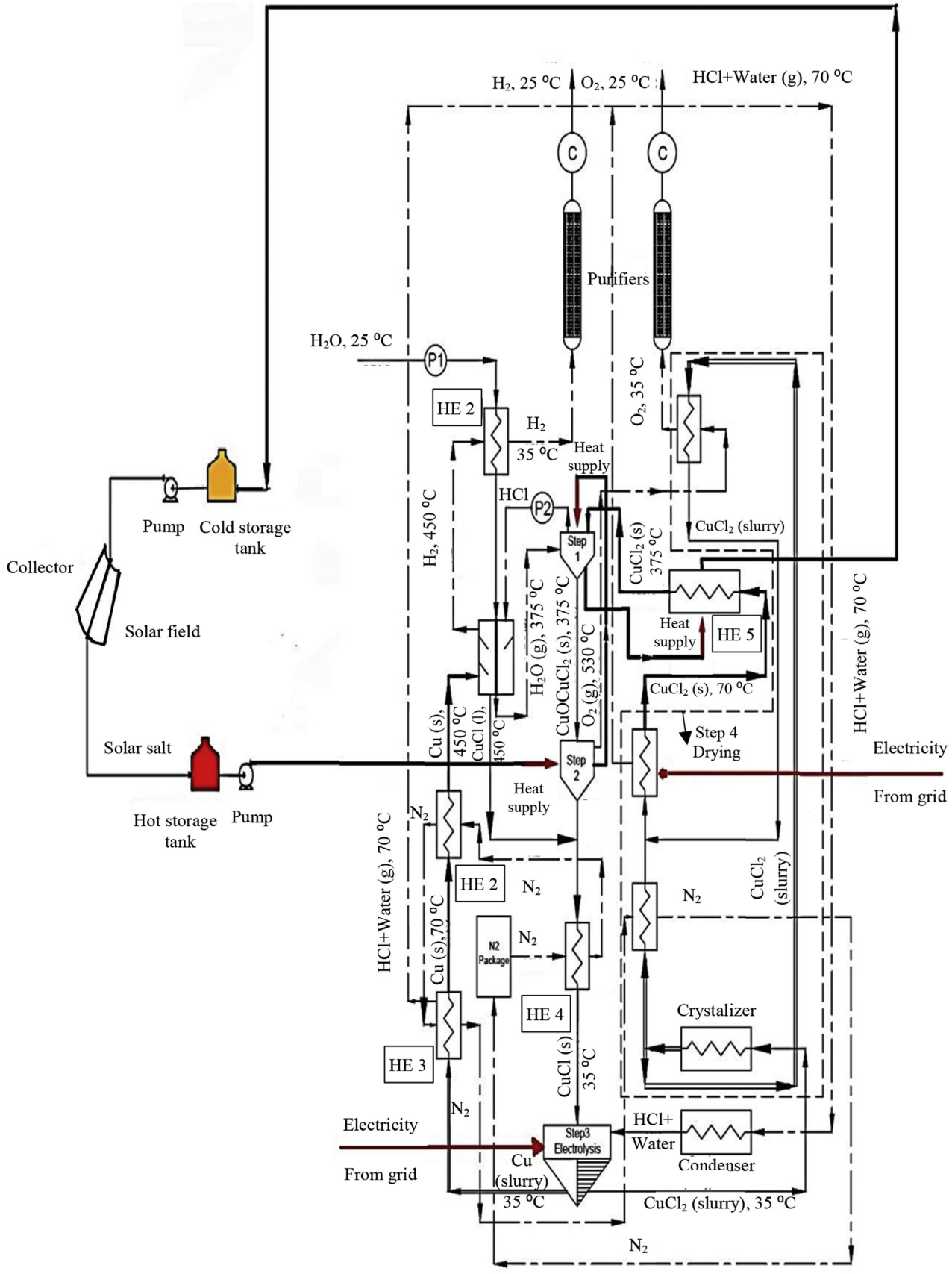

Fig. 5 – A Conceptual flowsheet for the modified solar CCC plant.

Table 3 – Specification of streams in the modified CCC plant.

Stream no.	Component	T (°C)	Flow rate (mol mol H_2^{-1})
1	H_2O	25	1
2	H_2O	25	1
3	H_2O	98	1
4	H_2	450	1
5	H_2	35	1
6	Cu(s)	450	2
7	HCl(g)	375	2
8	CuCl(l)	450	2
9	H_2O	375	1
10	CuCl(l)	530	2
11	CuCl(l)	490	4
12	CuCl(s)	35	4
13	N_2	25	11.5
14	N_2	480	11.5
15	$HCl + H_2O$	35	1
16	Cu(slurry)	35	2
17	$CuCl_2$(aq)	35	2
18	N_2	412	11.5
19	Cu	70	2
20	Cu	35	2
21	N_2	323	11.5
22	$CuCl_2$(s)	70	2
23	N_2	35	11.5
24	O_2	530	0.5
25	O_2	35	0.5
26	Solar salt	580	2.16
27	Solar salt	530	2.16
28	Solar salt	490	2.16
29	Solar salt	480	2.16
30	HCl	375	2
31	$CuOCuCl_2$	375	1
32	$CuCl_2$(aq)	375	2

cycle is related to the third step (electrolysis), and the other part is related to the fourth step (drying of the slurry of $CuCl_2$) that is not fully supplied by the heat recovered in the cycle. To provide the energy required by these two parts, the electrical energy can be used.

Comparison of the modified cycle Fig. 5 with the original cycle as given in Fig. 1 shows that in the original cycle, the inlet water to the cycle is divided into two parts. One part of that is heated by outlet hydrogen from the hydrogen production step and the other part by outlet oxygen from the oxygen production step for providing water steam required for the hydrolysis step. Comparison of thermal load of these three streams shows that delivered heat from hydrogen and oxygen streams is inadequate to increase the temperature of the inlet water from 25 °C to 375 °C. Hence in the modified cycle (Fig. 5), firstly, the total inlet water to the cycle is preheated by the outlet hydrogen from the fifth step and then receives the released heat of the hydrogen production step (fifth step reaction) until its temperature reaches the required temperature for the hydrolysis step. Another modification which has been performed in the preliminary cycle is using the nitrogen gas as an interface stream for exchanging the thermal energy between streams and recovering it. Energy efficiency of the cycles is calculated as follows:

$$\eta_{th.\ overall} = \frac{\overline{LHV}_{H_2}}{\sum \overline{Q}_{in} + \frac{\overline{E}}{0.4}} \quad (2)$$

In Eq. (2), $\overline{LHV}_{H_2}$ is defined as the molar lower heat value of the hydrogen that is equal to 241, 830 kJ $kmol^{-1}$. $\overline{Q}_{in}$ is the value of the input heat value for the cycle from an external heat source (solar energy) per mole of the hydrogen production. As mentioned earlier, due to average efficiency 0.7 for the collectors, this equates $Q_{cycle}/(0.7nH_2)$, where nH_2 is the molar rate of the produced hydrogen. Moreover, in Eq. (2), $\overline{E}/0.4$ is the equivalent heat of input electrical energy that is utilized in electrochemical, mechanical, electrical, separation, and so on, based on the conversion efficiency of thermal energy to electrical energy of 0.4. The amount of $\overline{E}/0.4$ for the CCC is nearly 62, 500 kJ kmol H_2^{-1} [11,12,19].

Table 4 shows the cold and hot utility requirements for both preliminary and modified cycle and compares their energy efficiency. As it is seen, the thermal efficiency in the modified cycle was increased about 10.1%. This efficiency will be improved further with the optimization process as will be presented in following sections.

Solar installations

Regarding various existing methods and systems to absorb the solar thermal energy, with respect to the range of operating temperatures in the thermo-chemical Cu–Cl hydrogen production cycle in which the maximum operating temperature is up to 530 °C, the best option is to use parabolic trough collector. Among existing technologies on a large scale, this system has been known the most trustworthy with the lowest cost [19]. Collectors' characteristic considered here was 100 m length and a span of 5.76 m. The maximum thermal efficiency with this type of collector is 0.79, where the mean annual thermal efficiency is 0.69. The distance between two rows of the collectors is a twice span of each collector so that the effect of shadows of the collectors can be minimized, and the available space optimized. As a result, available radiation on the collector spans is nearly 88% of Direct Normal Irradiation (DNI) of the solar energy.

A heat source is required to be delivered to the thermochemical CCC for continuing its hydrogen production during the day and night through the year. Therefore, to supply required heat for the cycle from solar energy, a storage unit shall be provided. A method to store solar heat is using two tanks for storage of hot and cold molten salt. When sunlight is strong enough, which can be used for heating the salt and supply of the required heat for the cycle, this salt is pumped

Table 4 – Comparison of the required hot and cold utility between early and modified cycles.

Parameters	Early cycle	Modified cycle
Hot utility (kJ $kmol\ H_2^{-1}$)	472.5	300.9
Cold utility (kJ $kmol\ H_2^{-1}$)	212.4	4.11
Thermal (energy) efficiency (%)	38.2	48.3

through the collector and after absorbing the solar energy enters the hot storage tank. Through the cycle, this salt is taken from the hot storage tank continuously and enters to the hydrogen production cycle and after providing required heat for the cycle, and cooling is returned to the cold tank. Again during the sunshine, this stream enters the solar installations and after the heat again is stored in the hot storage tank. This loop continues throughout the day and night. In the right-hand side of Fig. 5, a schematic of solar installation and hot/cold molten salt storage tanks was illustrated.

Model development

Thermodynamic model

General thermodynamic model of the plant's components
In this section, each step and component of the cycle were modeled under the following assumptions:

- Ambient temperature and pressure are considered as 25 °C and 1 *atm*, respectively.
- Temperature and pressure of reactants and products are equal to the reaction temperature
- Reactions are in steady state and adiabatic.

Chemical reactors. According to the first law of thermodynamics (conservation energy), in steady-state conditions, the transferred thermal energy to a chemical reaction in which no production or consumption of work happens is calculated by the following equation:

$$\dot{Q} = \sum_{P} \dot{H}_P - \sum_{R} \dot{H}_R = \sum_{P} \dot{n}\left(\overline{h}_f^0 + \overline{h} - \overline{h}_0\right) - \sum_{R} \dot{n}\left(\overline{h}_f^0 + \overline{h} - \overline{h}_0\right) \tag{3}$$

On the other hand, the exergy balance equation for this chemical reaction is:

$$\sum \dot{E}x_{in} - \sum \dot{E}x_{out} - \dot{E}x_d = \Delta Ex_{sys} \tag{4}$$

Specific exergy of a stream is:

$$\overline{ex} = \left(\overline{h} - \overline{h}_0\right) - T_0(\overline{s} - \overline{s}_0) + \overline{ex}^{CH} \tag{5}$$

By a combination of Eqs. (4) and (5):

$$\dot{E}x_d = \sum_{P} \dot{n}\left[\left(\overline{h} - \overline{h}_0\right) - T_0(\overline{s} - \overline{s}_0) + \overline{ex}^{CH}\right] - \sum_{R} \dot{n}\left[\left(\overline{h} - \overline{h}_0\right) - T_0(\overline{s} - \overline{s}_0) + \overline{ex}^{CH}\right] + \left(1 - \frac{T_0}{T_{reac.}}\right)\dot{Q} \tag{6}$$

In this equation, Q stands for the heat of reaction which for exothermic reactions is negative.

Heat exchangers. In heat exchangers, following equation can be used for calculation of the exergy destruction due to the heat transfer from a hot to a cold stream:

$$\dot{E}x_d = T_0\dot{Q}\frac{T_{ha} - T_{ca}}{T_{ha}T_{ca}} \tag{7}$$

The average thermodynamic temperatures respectively for hot and cold steam are T_{ha} and T_{ca} and are calculated as follows (in a constant pressure):

$$T_a = \frac{\overline{\overline{h}}_e - \overline{h}_i}{\overline{s}_e - \overline{s}_i} \tag{8}$$

Subscripts *i* and *e* stand for input and output streams, respectively. Furthermore, the heat exchanged between the hot and cold streams obtained from the following equation:

$$\dot{Q} = \left[\dot{n}\left(\overline{h}_e - \overline{h}_i\right)\right]_{cold} \tag{9}$$

Pumps. In the proposed plant as per Fig. 5, two pumps are considered. One of them is responsible for transferring the inlet water to the cycle, and the other one is for transferring of the produced hydrochloric acid. Thermodynamic analysis of these pumps can be performed easily by applying the first and second law of thermodynamics.

Thermodynamic model of the solar installation
The solar installation the CCC, and used to provide the required heat for the cycle. As described before, this facility consists of a series of parabolic collectors which absorb thermal energy from the sun and two storage tanks for hot and cold molten salt. No chemical reaction happens in these facilities, and only heat transfer takes place to the molten salt. Considering stream numbers listed in Table 4, heat balance and exergy destruction equations are as follows:

$$\dot{Q} = \dot{n}_{26}\left(\overline{h}_{26} - \overline{h}_{29}\right) \tag{10}$$

and:

$$\dot{E}x_d = \dot{n}_{26}\left[\left(\overline{h}_{26} - \overline{h}_{29}\right) - T_0(\overline{s}_{29} - \overline{s}_{26})\right] + \left(1 - \frac{T_0}{T_{ca}}\right)\dot{Q} \tag{11}$$

where T_{ca} stands for the average thermodynamic temperature of the molten salt:

$$T_{ca} = \frac{\overline{h}_{26} - \overline{h}_{29}}{\overline{s}_{26} - \overline{s}_{29}} \tag{12}$$

Now the stored energy in the hot tank can be calculated. The received thermal energy from the sun is indicated as $\Phi(t) \geq 0$, and the delivered heat (without disruption and definitive) to Cu–Cl thermochemical cycle is considered $Q_{cycle}(t) \geq 0$. Hence, the stored energy is:

$$\frac{dS}{dt} = \Phi(t) - Q_{cycle}(t) \tag{13}$$

The stored energy in at the specific time of day is obtained by integrating Eq. (13) as follows:

$$S(t_1) = \int_{t_0}^{t_1}\left[\Phi(t) - Q_{cycle}(t)\right]dt + S(t_0) \tag{14}$$

S (t_{min}) or S_{min} stand for the least capacity of the stored energy and S (t_{max}) or S_{max} denotes the highest value of the stored energy during 24 h; therefore, their difference represents the amount of stored energy in a hot tank of molten salt during that period of time:

$$Q_{reserve} = S_{max} - S_{min} \quad (15)$$

S_{max} and S_{min} values can be obtained by solving the equation $dS/dt = \Phi(t) - Q_{cycle}(t) = 0$ where $\Phi(t) = Q_{cycle}(t)$. In other words, the minimum stored energy in the hot tank during 24 h can occur when the amount of received energy from the sunshine by the solar installations is equal to the amount of required energy by the thermochemical cycle. This situation happens twice a day. One in the morning when the sunrise intensity is increasing, and the received solar energy is equivalent to the energy delivered to the cycle. This time is the moment of t_{min}, before this time, the received energy from the sun is zero during the night, and the entered energy to the cycle is delivered from the hot storage tank. So the stored energy in the hot tank is steadily declining during the night. After this moment (t_{min}), the received energy from the sun is more than the required energy of the cycle. Therefore, the excess energy is stored in the hot tank of molten salt. This storage is increasing continuously until the sunset on the evening, which the thermal energy received from the sun is equal to the heat requirements by the cycle again. This moment is the time of maximum stored thermal energy is in the hot tank, i.e. t_{max}. At the end of the day, the sunshine tends to zero and the required heat by the cycle is provided from the stored energy in the hot tank of molten salt again.

Regardless of that short period of times between t_{max}, and t_{min} in which $\Phi(t) = 0$ (e.g. due to the bad weather), maximum capacity of the stored heat per day is calculated as follows:

$$Q_{reserve} = S_{max} - S_{min} = \int_{t_{max}}^{t_{min}+24} Q_{cycle}(t)dt \quad (16)$$

In which $t_{max} < t < t_{min} + 24$. Hence, between the evenings when the sun sets until the next morning when the sun rises, the value of $\Phi(t)$ (sunshine) is zero; therefore, the stored energy shall supply the required energy for the cycle. If the required thermal power to be delivered to the cycle was constant, e.g. $Q_{cycle}(t) = Q_0$, then the required heat of the cycle during the night is:

$$Q_{cycle} = Q_0\left[1 - \frac{(t_{max} - t_{min})}{24}\right]24 \quad (17)$$

During the night $\Phi(t) = 0$ and $Q_{cycle}(t) > 0$, hence, S(t) decreases until its amount reaches to the S_{min} in the time of t_{min}. The minimum storage point is during the sunrise and can deliver thermal power, which is equal to the required thermal power for the cycle. The maximum stored energy occurs when the solar thermal power is falling back into the state that $\Phi(t) = Q_{cycle}(t)$ is reached. Considering the solar efficiency of the collector as $\eta_{col} = 0.7$, the absorbed solar heat by the collector, at any given time, t, is obtained as:

$$\Phi(t) = \eta_{col} I_c \quad (18)$$

where I_c is the received radiant energy from the son by the solar collector. Calculation procedure for I_c was given in Ref. [31].

The aim of this project is to provide the thermal requirement of the Cu–Cl thermochemical cycle using solar thermal energy in a city like as Tehran-Iran.

Energy efficiency. Overall energy efficiency of thermochemical CCC is defined as a portion of energy supplied, which is recoverable by the latent energy of the produced hydrogen. As explained in the introduction, electrolysis is one of the steps in the Cu–Cl thermochemical cycle (Cu production step) in which electrical energy is employed. Furthermore, in some conducted researches, the heat required in the chemical reaction is considered as input for this step and in some others, electrical energy is considered as input [25]. In the present study, the electrical energy is considered as input energy. Therefore, the overall energy efficiency is calculated by Eq. (2):

Exergy efficiency. Overall exergy efficiency of the CCC is defined as a portion of exergy supplied, which is recoverable by the chemical exergy of the produced hydrogen:

$$\eta_{ex.overall} = \frac{\overline{ex}^{CH}_{H_2}}{\overline{E} + \sum\left(1 - \frac{T_0}{T_{reac}}\right)\overline{Q}_{reac}} \quad (19)$$

In Eq. (19), $\overline{ex}^{CH}_{H_2}$ is the chemical exergy of the hydrogen which is 320, 822 kJ $kmol^{-1}$.

Thermoeconomic model

In developing the thermoeconomic model, the economic analysis was performed based on the total revenue requirement, TRR, method, as given in Refs. [32,33].

Generally, cost balance equations of each component of the system are formulated, separately. If k is an index that denotes the kth component in an energy system while *n* exergy streams flow into that component and m exergy streams exit from the proposed component; then, the cost balance for the proposed kth component suggests that the overall cost outflows are equivalent to the cost of outflows plus the associated costs of the capital investment and operation & maintenance cost of the kth component. Hence, we have:

$$\sum_{j=1}^{n}\left(c_j \dot{E}x_j\right)_{k\cdot i} + \dot{Z}_k = \sum_{j=1}^{m}\left(c_j \dot{E}x_j\right)_{k\cdot e} \quad (20)$$

Exergy rates of input and output from the kth component are obtained using the exergy analysis. In thermoeconomic (exergoeconomic) analysis of a component, it is assumed that the unit costs of inflow's exergies are known, and the aim is calculating the unit cost of outflow's exergies (the unit costs of outflow's exergies are unknowns). When there is only one outflow exergy, Eq. (20) is solved and the one unknown cost is calculated; however, when the number of outflows is ≥2, the number of unknowns is more than the number of equation (there is only one cost balance equation). In such case, auxiliary cost equations are defined to increase the number of the equation equal to the number of unknown variables. There are two categories of auxiliary cost equations that obtained based on so-called F and P rules. More, details on these rules were given in Ref. [32].

The cost balance equation (Eq. (20)) and auxiliary equations (when they are necessary) were implemented on various components of the proposed CCC plant (that was depicted in

Fig. 5). The cost rate of capital investment and operating and maintenance.

In Eq. (20), $\dot{Z}_k$ is associated cost of the capital investment and operating and maintenance cost of kth component of the proposed plant. This parameter was obtained as:

$$\dot{Z}_k = \dot{Z}_k^{CI} + \dot{Z}_k^{OM} = \left[\frac{CC_L + OMC_L}{\tau}\right]\left(\frac{PEC_k}{\sum PEC_K}\right) \quad (21)$$

where CC_L and OMC_L are the levelized carrying charge and operating and maintenance cost, respectively. τ is the total annual operating hours of the component assumed as $\tau = 0.85 \times 8760 = 7446$ h (assuming that the system is in service at 85% of the annual time). Procedure for calculating CC_L and OMC_L were given in Refs. [32,33]. In Eq. (21), it was assumed that the total investments of the plant can be apportioned to each component according to the share of the purchased cost of that component in the total purchased equipment cost of the overall system (plant). The purchased equipment cost of the kth component, PEC_k, for components of the solar CCC was obtained based on the following section.

Purchased equipment cost of the solar CCC

Chemical reactors. The purchased equipment costs of chemical reactors were approximated using [4]. In this regard we have:

$$PEC_{step1} = 1.06 \times \left(-7.936 \times 10^{-5}\dot{V}_{CuCl_2} + 1.565\dot{V}_{CuCl_2} + 5489.6\right) \quad (22)$$

1.06 in the right-hand side of Eq. (22) is a coefficient that was considered for the effect of special coatings. $\dot{V}_{CuCl_2}$ is the volumetric flow rate of $CuCl_2$ in L min^{-1}

$$PEC_{step2\&step5} = 1.989 \times 10^{-3} q_{step2} + 60.421 \quad (23)$$

q_{step2} is the thermal capacity of reactors in MW.

Third to the fifth step can be approximated by the electrolyser section of [5].

$$PEC_{step3} = 2500 \times A_{step3} \times \varepsilon \quad (24)$$

where, ε is the activity coefficient. In the present study, it was assumed to be 0.95. In addition, we have:

$$\begin{aligned} A_{shell} &= \pi D_{inside} \times L \\ A_{head} &= \pi\left(\frac{D_{inside}}{2}\right)^2 \\ A_{step3} &= A_{shell} + (2 \times A_{head}) \end{aligned} \quad (25)$$

The reactor was assumed to be $D_{inside} = 3\ m$ and $L = 10\ m$.

As previously mentioned, the fourth step of the cycle is the only step where the chemical reaction does not occur. The fourth step is a spray-dryer reactor type. To calculate the purchase price of the dryers, we have [31]:

$$PEC_{step4} = 240.47 \times A_{step4} + 22607 \quad (26)$$

Heat exchangers and pumps. For other equipment, including heat exchangers and pump empirical correlations given in Ref. [33] was used to estimate the purchased equipment cost of them. For example, for heat exchangers, the heat-transfer areas were estimated using LMTD method and the final cost of each heat exchanger was estimated as a function of its heat-transfer area using graphs and/or correlations given in Ref. [33]. For pumps, the purchased equipment cost is usually given in terms of the kW or hp of the pump using empirical correlation. In this regards, refer to [34].

Solar facilities. For parabolic trough solar collectors, the purchase cost is 2000–3000 \$ kW^{-1} [35]. In addition, a significant amount of investment should be paid for the storage tank. For storage tank we have [34]:

$$PEC_{Tank} = 5.0127\ L^{-0.1931} \quad (27)$$

In the above equation, L stands for the tank volume in liters. Finally, 12% of the total annual costs of the collector and tank was considered for valves, pumps, and control equipment [34]. In addition, more 5% were added to consider the cost of installation, calibration and adjustment of collectors.

Optimization

Objective functions

The aim of optimization in this paper is maximizing the energy efficiency, exergy efficiency and minimizing the cost of hydrogen production. Four optimization scenarios were conducted. In three scenarios, each aforementioned objective was optimized with a single-objective optimization approach, while in the fourth scenario, all objectives were optimized simultaneously in a multi-objective optimization process. The mathematical formulations of these three objective functions, including energy efficiency, exergy efficiency and the unit cost of hydrogen production for the proposed CCC plant were given in Eq. (28a)–(28c), respectively.

Objective #1: Energy Efficiency

$$\eta_{ex.overall} = \frac{\overline{ex}_{H_2}^{CH}}{\overline{E} + \sum\left(1 - \frac{T_0}{T_{reac}}\right)\overline{Q}_{reac}} = 1 - \frac{\overline{Ex}_d}{\overline{E} + \sum\left(1 - \frac{T_0}{T_{reac.}}\right)\overline{Q}_{reac.}} \quad (28a)$$

Objective #2: Exergetic Efficiency

$$\eta_{th.\ overall} = \frac{\overline{LHV}_{H_2}}{\sum \overline{Q}_{in} + \frac{\overline{E}}{0.4}} \quad (28b)$$

Objective #3: The cost of each kilogram of the produced hydrogen

$$c_{H_2} = c_4\ \overline{ex}_{H_2}^{CH} \quad (28c)$$

In Eq. (28a), $\overline{Ex}_d$ is total exergy destruction of the CCC plant per mole of hydrogen production. In Eq. (28c), c_4 is the cost of outflow exergy of the hydrogen from fifth step reactor as per Fig. 5 and stream numbers indicated in Table 3. It was multiplied with $\overline{ex}_{H_2}^{CH}$ to convert its unit from \$ kJ^{-1} into \$ kg^{-1}.

Decision variables and constraints

In order to optimize objective functions presented as Eqs. (29a)–(29c), operating temperature of the five main reactions

(steps 1–5) along with the number of the solar collectors and volume of the solar storage tank were chosen as decision variables. It was assumed that the optimization is subject to the following constraints [5,19].

$$300 \leq T_{step1} \leq 400°C \quad (29a)$$

$$480 \leq T_{step2} \leq 550°C \quad (29b)$$

$$35 \leq T_{step3} \leq 70°C \quad (29c)$$

$$70°C \leq T_{step4} \quad (29d)$$

$$430 \leq T_{step3} \leq 475°C \quad (29e)$$

Optimization method

In the fourth scenario (multi-objective scenario) a special type of genetic algorithm called as the non-dominated sorting genetic algorithm, NSGA-II, was employed. Detail regarding NSGA-II was given in Refs. [36,37]. In multi-objective optimizations instead of having a single final optimal solution, there is a set of optimal solution locating on a frontier of solutions called as the Pareto frontier. Hence, a process of decision-making is required to select a single final optimal result among available solutions. One easy and efficient method for this purpose is using TOPSIS-Technique for Order of Preference by Similarity to Ideal Solution method. More details of the formulation of the TOPSIS were given in Refs. [37,38].

Results

As mentioned in previous sections, four optimization scenarios were performed on the three objective functions of the proposed solar CCC plant (illustrated in Fig. 5) that produces 6000 kg of hydrogen per day. Those objectives that were indicated by Eqs. (28a)–(28c) were optimized based on decision variables mentioned in "Decision variables and constraints" Section and constraints as indicated by Eqs. (29a)–(29e). Four optimization scenario were performed. In the three scenarios, each objective function was optimized separately regardless of other objectives (single-objective optimization). In the fourth scenario (multi-objective optimization), the three objectives were optimized simultaneously using the NSGA-II algorithm. As mentioned in "Optimization method" Section, in the multi-objective scenario, the Pareto frontier of the optimal solution is obtained instead of a single final optimal solution of single-objective scenarios. The Pareto frontier of the fourth optimization scenario of the solar CCC plant was illustrated in Fig. 6.

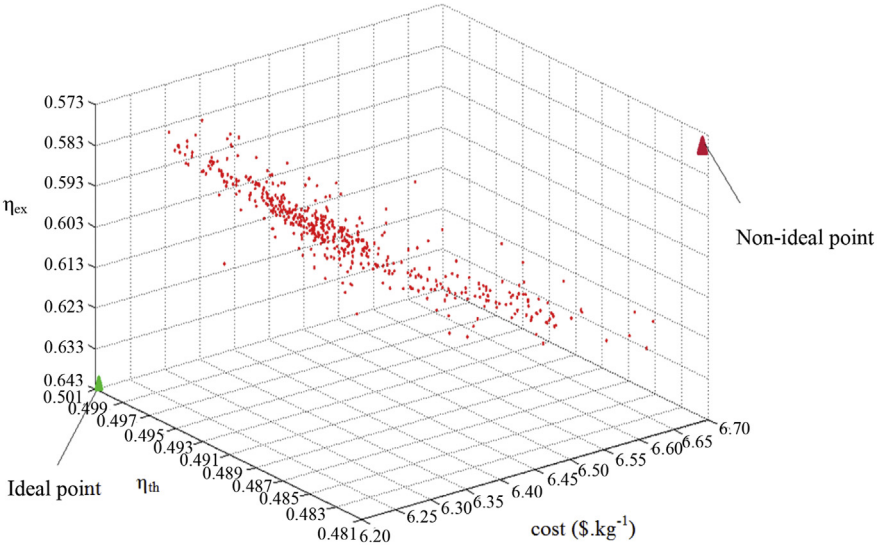

Fig. 6 – Pareto optimal frontier in multi-objective optimization scenario with objectives of hydrogen production cost, thermal efficiency and exergy efficiency.

Table 5 – Decision variables at the base case and four optimizes systems.

Decision variables	Base case	En. optimized	Ex. optimized	Cost optimized	Multi-obj.
T_1 (°C)	375.0	336.0	314.0	328.0	328.0
T_2 (°C)	530.0	524.0	507.0	487.0	489.0
T_3 (°C)	35.0	26.0	64.0	54.0	42.0
T_4 (°C)	70.0	148.0	143.0	105.0	147.0
T_5 (°C)	450.0	430.0	469.0	442.0	441.0
No. of solar collector	187	176	182	178	178
Volume of molten salt (m^3)	2108	2060	1750	1600	170

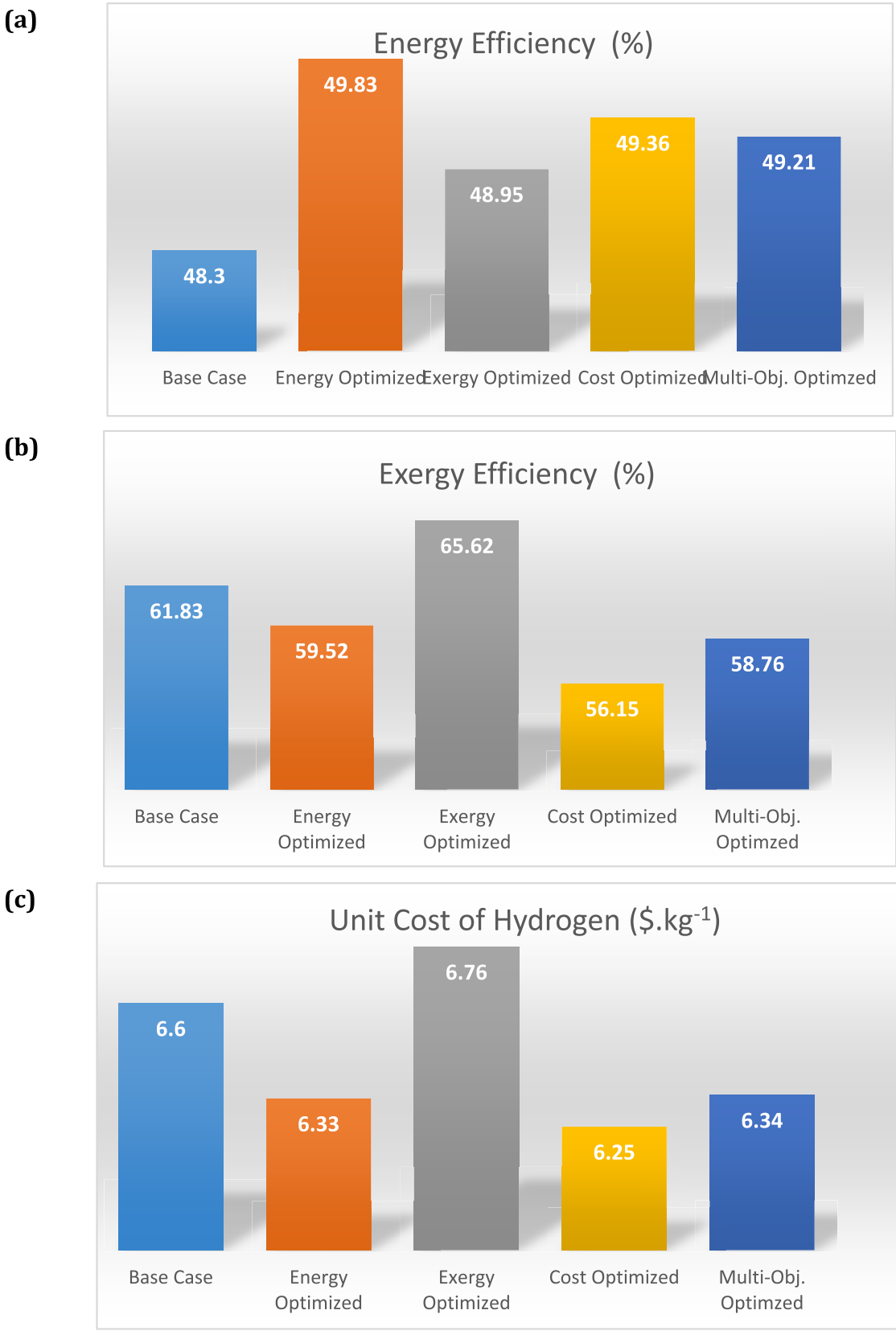

Fig. 7 – Comparison of the objective functions of the base case and various optimized scenarios (a) Energy efficiency; (b) Exergy efficiency; (c) The unit cost of produced hydrogen.

It is clear from this figure that by increasing energy efficiency, the unit cost of the produced hydrogen will decline; however, with increasing the exergy efficiency, this cost will increase to an extent that the increase of the exergy efficiency is not cost-effective. To decide on the best option using the TOPSIS (described in "Optimization method" Section); first of all, the ideal and non-ideal solution must be specified. Obviously, the ideal solution having the lowest cost, highest thermal efficiency, and highest energy efficiency; the non-ideal solution has the maximum production cost, the lowest thermal efficiency, and the lowest exergy efficiency. The ideal and non-ideal solutions were indicated on the lower-right and upper-left corners of Fig. 6. Eventually, the TOPSIS decision-making method was employed to choose a final optimal solution from Fig. 6 in the fourth scenario.

Table 5 compares the values of decision variables of the four optimization scenario with the base case CCC plant that was designed in "Conceptual design and heat recovery in the solar thermochemical cycle" Section.

For better insight regarding objective functions (thermal and exergetic efficiencies and hydrogen cost), Fig. 7a–c were presented here to compare these criteria of various designs, including the base case system (as per "Conceptual design and heat recovery in the solar thermochemical cycle" Section) and four optimized plants.

As per these figures, the maximum attainable energy and exergy efficiency are 49.84% and 58.23%, respectively. This figure for the minimum cost of produced hydrogen is 6.24 \$ kg^{-1}. The ideal design should have these features for all objectives; however, as per Fig. 7a–c, clearly it is impossible to have this feature in four optimized scenarios as well as the base case system. In addition, according to Fig. 7a–c it can be found that the worst design may have 48.31% and 58.62% for energy and exergy efficiency, respectively and 6.76 \$ kg^{-1} for the unit cost of the produced hydrogen. Hence, this is a feature of the non-ideal design. The five designs of the solar CCC plant (one base case plus four optimized systems) have features between these two ideal and non-ideal extremes. Now, a question is which designs is more desired among available five. This question can be answered using implication of the TOPSIS decision-making method one more. If magnitudes of objectives of all options are normalized and special distance of each design from the ideal and non-ideal designs are denoted by d^+ and d^-, then option having the biggest value of $C = d^-/(d^+ + d^-)$ i.e. having largest deviation from the non-ideal and smallest deviation from the ideal, is the most desired feature. This analysis was performed for all alternatives, and its results were summarized in Table 6.

As it is clear from Table 6, the energy-optimized system has maximum C factor; therefore, it was selected as the final desired optimized solar CCC plant. The final specifications of the desired solar CCC plant were summarized in Table 7.

The final suggested solar CCC plant (with specifications that were mentioned in Table 7, and a flowsheet as per Fig. 5) has a thermal efficiency of 49.84%. If this thermal efficiency is compared with the conceptual design of [19], it can be found that this efficiency was improved 11.64%. 10.1% of this improvement was due to the heat recovery as per "Conceptual design and heat recovery in the solar thermochemical cycle" Section and remainder (1.44%) was obtained through the optimization. The maximum efficiency of a three-step CCC through the heat integration was previously obtained by Wu et al. [16] to be 47.31%. Our designed and optimized system has a 2.53% more thermal efficiency. The exergetic efficiency of this system is 58.23% (−0.39% lower than the base case), and its unit cost of hydrogen production is 6.33 \$ kg^{-1} (4.3% lower than the base case).

For better insight into the role of the investment cost of the solar installation, a total investment of the CCC plant, and solar installation as a fraction of the total investment, Fig. 8a–c were presented here.

Table 6 – TOPSIS criteria of various designs of the solar CCC plant.

Option	En. eff. (%)	Ex. eff. (%)	c_{H2} (\$ kg^{-1})	Normalized en. eff.	Normalized ex. eff.	Normalized cH_2	d^+	d^-	C
Base case	48.31	58.62	6.60	0.3706	0.3795	0.3853	0.0296	0.0579	0.6620
En. optimized	**49.84**	**58.23**	**6.33**	**0.3844**	**0.3766**	**0.3696**	**0.0198**	**0.1321**	**0.8697**
Ex. optimized	48.96	60.84	6.76	0.3765	0.3958	0.3947	0.0308	0.0334	0.5199
Cost optimized	49.37	56.31	6.25	0.3802	0.3625	0.3649	0.0336	0.1468	0.8136
Multi-obj. optim.	49.22	57.54	6.34	0.3788	0.3715	0.3702	0.0255	0.1004	0.7975
Ideal	49.84	60.84	6.25	0.3844	0.3958	0.3649	0.0000	0.1505	1.0000
Non-ideal	48.31	56.31	6.76	0.3706	0.3625	0.3947	0.0468	0.0000	0.0000

Bold data belongs to the final selected scenario.

Table 7 – Final features of the selected solar CCC plant (based on conceptual design of Fig. 7).

En. eff. (%)	Ex. eff. (%)	cH_2 (\$ kg^{-1})	T_1 (°C)	T_2 (°C)	T_3 (°C)	T_4 (°C)
49.83	51.13	6.33	336.0	524.0	26.0	148.0

T_5 (°C)	ΔT_{pinch} (°C)	No. of solar collector	Solar storage tank volume (m^3)	Capital investment (MM\$)	Capital investment of solar installation (MM\$)
430	30.0	176	2060.0	39.20	16.59

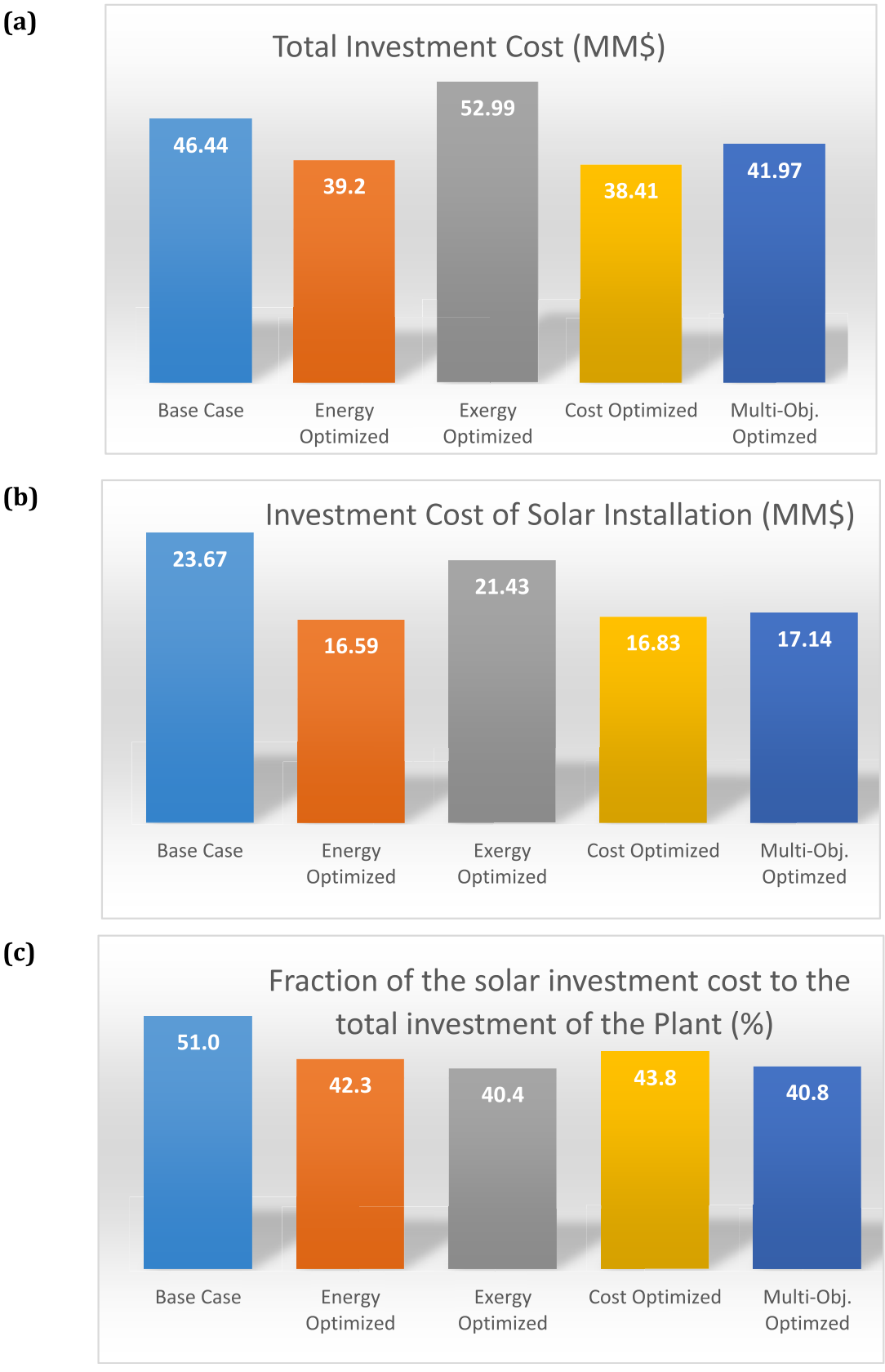

Fig. 8 – Comparison of the (a) Total investment cost (MM$); (b) Investment cost of the solar installation (MM$); (c) Fraction of the investment cost of solar installation to the total investment (%).

As per Fig. 8a and b, the investment cost of the final selected plant (energy optimized system) is 39.20 MM$ including 16.59 MM$ for an investment cost of the solar installation. This investment cost is 13.5% higher than the base case system. It is clear that the investment cost of the solar installation is 42.3% of the total investment for the case of optimum thermal (energy) efficiency (see Fig. 8c). These costs are based on the total production capacity of 6000 kg day^{-1}. Comparing the share of the solar installation in the total investment cost of the plant reveals that the minimum share belongs to exergy optimized system with 40.4% and maximum share belongs to the base case system with 51.0% (see Fig. 8c). The average share of the solar installation in total investment cost of the CCC plant is almost 43.7% which is a reasonable value. The concern should be done to reduce this cost to make a more economic sound Cu–Cl thermochemical hydrogen production plant. In this regard, if the economic criteria are the only concern of designers, the economic-optimized system can be selected that having 6.25 $ kg^{-1} (5.3% lower than the base case) with the investment of 38.41 MM$ (17.3% cheaper than the base case). Nevertheless, in this plant the share of the solar installation in the total investment cost of the plant is 43.8%.

Conclusion

The conceptual design of a solar Cu–Cl thermochemical hydrogen production plant with a capacity of 6000 kg per day was presented by considering heat recovery between hot and cold streams. A heat exchanger network was designed based on the pinch analysis, and the thermal efficiency of the proposed cycle was improved about 10.2%. This conceptual design was considered as the base case system for further improvement using optimization tools if several optimization scenarios. Objective functions were the energy efficiency, exergy efficiency, and the unit cost of produced hydrogen. It was found that the most desired system was the system that was optimized based on the maximum thermal efficiency in a single-objective optimization approach. It was found that this improved the efficiency of the previously modified system +1.53% compared to previously process integrated system (the bae case system). The comparison between modified thermal efficiency by the process integration (heat recovery) and optimization implied that the heat recovery is very more effective than optimization, and it should be considered in the design of any CCC plant. The final recommended system had 49.84% thermal efficiency, 58.23% exergetic efficiency and 6.33 $ kg^{-1} for produced hydrogen. The capital cost of the suggested plant was 39.20 MM$ including 16.59 MM$ for the solar installation. The average share of the solar installation on the total investment cost of the solar CCC plant was 43.7% implying that any attempt to make this plant more economic, should be paid on reducing the cost of the solar installation.

Acknowledgement

This is to acknowledge the effective attempt of Mr. Ali Sohani in providing and editing art works, formulas, and references' list. Moreover, received assists of Ms. Parastoo Fahimpour is highly appreciated.

REFERENCES

[1] Liu K, Song C, Subramani V. Hydrogen and syngas production and purification technologies. Wiley Online Library; 2010.
[2] Nikolaidis P, Poullikkas A. A comparative overview of hydrogen production processes. Renew Sustain Energy Rev 2017;67:597–611.
[3] Balta MT, Dincer I, Hepbasli A. Comparative assessment of various chlorine family thermochemical cycles for hydrogen production. Int J Hydrogen Energy 2016;41(19):7802–13.
[4] Lewis MA, Ferrandon MS, Tatterson DF, Mathias P. Evaluation of alternative thermochemical cycles – Part III further development of the Cu–Cl cycle. Int J Hydrogen Energy 2009;34(9):4136–45.
[5] Orhan MF. Energy, exergy and cost analyses of nuclear-based hydrogen production via thermochemical water decomposition using a copper-chlorine (Cu–Cl) cycle. 2008.
[6] Orhan MF, Dincer I, Naterer GF. Cost analysis of a thermochemical Cu–Cl pilot plant for nuclear-based hydrogen production. Int J Hydrogen Energy 2008;33(21):6006–20.
[7] Orhan MF, Dincer I, Rosen MA. Exergoeconomic analysis of a thermochemical copper–chlorine cycle for hydrogen production using specific exergy cost (SPECO) method. Thermochim Acta 2010;497(1–2):60–6.
[8] Orhan MF, Dincer I, Rosen MA. Efficiency analysis of a hybrid copper–chlorine (Cu–Cl) cycle for nuclear-based hydrogen production. Chem Eng J 2009;155(1–2):132–7.
[9] Ozbilen A, Dincer I, Rosen MA. Development of a four-step Cu–Cl cycle for hydrogen production – Part I: exergoeconomic and exergoenvironmental analyses. Int J Hydrogen Energy 2016;41(19):7814–25.
[10] Ozbilen A, Dincer I, Rosen MA. Development of a four-step Cu–Cl cycle for hydrogen production – Part II: multi-objective optimization. Int J Hydrogen Energy 2016;41(19):7826–34.
[11] Naterer G, Suppiah S, Lewis M, Gabriel K, Dincer I, Rosen MA, et al. Recent Canadian advances in nuclear-based hydrogen production and the thermochemical Cu–Cl cycle. Int J Hydrogen Energy 2009;34(7):2901–17.
[12] Daggupati VN, Naterer GF, Gabriel KS, Gravelsins RJ, Wang ZL. Equilibrium conversion in Cu–Cl cycle multiphase processes of hydrogen production. Thermochim Acta 2009;496(1–2):117–23.
[13] Momirlan M, Veziroglu TN. Current status of hydrogen energy. Renew Sustain Energy Rev 2002;6(1–2):141–79.
[14] Rabbani M, Dincer I, Naterer GF, Aydin M. Determining parameters of heat exchangers for heat recovery in a Cu–Cl thermochemical hydrogen production cycle. Int J Hydrogen Energy 2012;37(15):11021–34.
[15] Pope K, Wang Z, Naterer GF. Process integration of material flows of copper chlorides in the thermochemical Cu–Cl cycle. Chem Eng Res Des 2016;109:273–81.
[16] Wu W, Chen HY, Wijayanti F. Economic evaluation of a kinetic-based copperchlorine (CuCl) thermochemical cycle plant. Int J Hydrogen Energy 2016;41(38):16604–12.
[17] Jaszczur M, Rosen MA, Śliwa T, Dudek M, Pieńkowski L. Hydrogen production using high temperature nuclear reactors: efficiency analysis of a combined cycle. Int J Hydrogen Energy 2016;41(19):7861–71.
[18] Wang Z, Naterer GF, Gabriel KS, Secnik E, Gravelsins R, Daggupati V. Thermal design of a solar hydrogen plant with a

copper–chlorine cycle and molten salt energy storage. Int J Hydrogen Energy 2011;36(17):11258–72.
[19] Ghandehariun S, Naterer GF, Dincer I, Rosen MA. Solar thermochemical plant analysis for hydrogen production with the copper–chlorine cycle. Int J Hydrogen Energy 2010;35(16):8511–20.
[20] Ghandehariun S, Rosen MA, Naterer GF, Wang Z. Comparison of molten salt heat recovery options in the Cu–Cl cycle of hydrogen production. Int J Hydrogen Energy 2011;36(17):11328–37.
[21] Jaber O, Naterer GF, Dincer I. Heat recovery from molten CuCl in the Cu–Cl cycle of hydrogen production. Int J Hydrogen Energy 2010;35(12):6140–51.
[22] Yildiz B, Kazimi MS. Efficiency of hydrogen production systems using alternative nuclear energy technologies. Int J Hydrogen Energy 2006;31(1):77–92.
[23] Ghandehariun S, Rosen MA, Naterer GF. Direct contact heat transfer from molten salt droplets in a thermochemical water splitting process of hydrogen production. Int J Heat Mass Transf 2016;96:125–31.
[24] Hosseini SE, Wahid MA. Hydrogen production from renewable and sustainable energy resources: promising green energy carrier for clean development. Renew Sustain Energy Rev 2016;57:850–66.
[25] Ratlamwala TAH, Dincer I. Comparative energy and exergy analyses of two solar-based integrated hydrogen production systems. Int J Hydrogen Energy 2015;40(24):7568–78.
[26] Yilmaz F, Balta MT, Selbaş R. A review of solar based hydrogen production methods. Renew Sustain Energy Rev 2016;56:171–8.
[27] Dincer I, Acar C. Review and evaluation of hydrogen production methods for better sustainability. Int J Hydrogen Energy 2015;40(34):11094–111.
[28] Turner J, Sverdrup G, Mann MK, Maness PC, Kroposki B, Ghirardi M, et al. Renewable hydrogen production. Int J Energy Res 2008;32(5):379–407.
[29] Yuksel YE, Ozturk M. Thermodynamic and thermoeconomic analyses of a geothermal energy based integrated system for hydrogen production. Int J Hydrogen Energy 2017;42(4):2530–46.
[30] Lewis MA, Masin JG, O'Hare PA. Evaluation of alternative thermochemical cycles, Part I: the methodology. Int J Hydrogen Energy 2009;34(9):4115–24.
[31] Goswami DY, Kreith F, Kreider JF. Principles of solar engineering. CRC Press; 2000.
[32] Bejan A, Tsatsaronis G. Thermal design and optimization. John Wiley & Sons; 1996.
[33] Sayyaadi H. Multi-objective approach in thermoenvironomic optimization of a benchmark cogeneration system. Appl Energy 2009;86(6):867–79.
[34] Peters MS, Timmerhaus KD. Plant design and economics for chemical engineers. 4th ed. McGraw-Hill, Inc.; 1991. chemical engineering series.
[35] Eicker U. Solar technologies for buildings. John Wiley & Sons; 2006.
[36] Sayyaadi H, Aminian HR. Multi-objective optimization of a recuperative gas turbine cycle using non-dominated sorting genetic algorithm. Proc Institution Mech Eng Part A J Power Energy 2011. 0957650911420930.
[37] Sohani A, Sayyaadi H, Hoseinpoori S. Modeling and multi-objective optimization of an M-cycle cross-flow indirect evaporative cooler using the GMDH type neural network. Int J Refrig 2016;69:186–204.
[38] Sayyaadi H, Mehrabipour R. Efficiency enhancement of a gas turbine cycle using an optimized tubular recuperative heat exchanger. Energy 2012;38(1):362–75.
[39] Naterer GF, Gabriel K, Wang ZL, Daggupati VN, Gravelsins R. Thermochemical hydrogen production with a copper–chlorine cycle. I: oxygen release from copper oxychloride decomposition. Int J Hydrogen Energy 2008;33(20):5439–50.